Supporting Information

Facile biofabrication of heterogeneous multilayer tubular hydrogels by fast diffusion-induced gelation

Liliang Ouyang[1,4], Jason A. Burdick[2], Wei Sun[1,3,*]

[1] Department of Mechanical Engineering, Tsinghua University, Beijing 100084, China
[2] Department of Bioengineering, University of Pennsylvania, Philadelphia, PA 19104, USA
[3] Department of Mechanical Engineering and Mechanics, Drexel University, Philadelphia, PA 19104, USA
[4] Present address: Department of Materials, Imperial College London, London, SW7 2AZ, UK
*Email: weisun@tsinghua.edu.cn

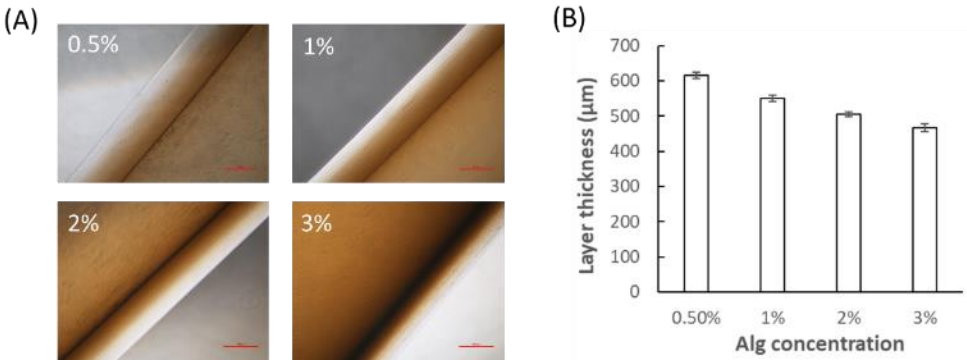

Figure S1. Effect of alginate concentration on layer thickness. (A) Microscopy images and (B) quantification of the coated alginate layer with alginate concentrations of 0.5 to 3%. Scale bar: 500µm.

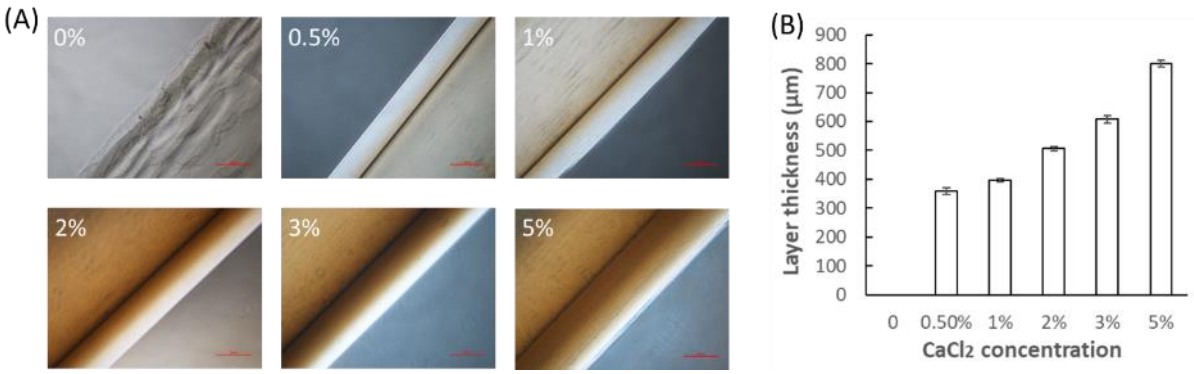

Figure S2. Effect of $CaCl_2$ concentration on layer thickness. (A) Microscopy images and (B) quantification of the coated alginate layer with $CaCl_2$ concentrations of 0 to 5%. Scale bar: 500µm.

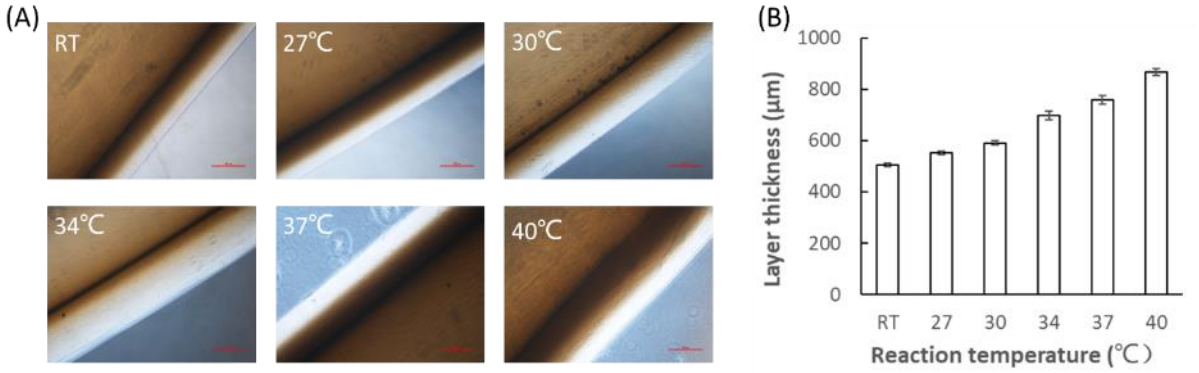

Figure S3. Effect of reaction temperature on layer thickness. (A) Microscopy images and (B) quantification of the coated alginate layer with temperatures from room temperature (RT) to 40°C. Scale bar: 500µm.

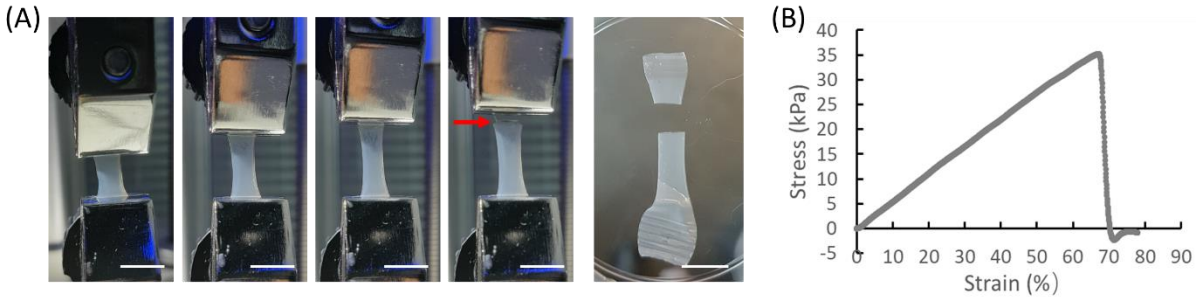

Figure S4. (A) Tensile test process showing sample fracture (red arrow) and the broken tubular structure (reaction time was 1 min during preparation) after testing. (B) Representative stress-strain curve of tensile test based on alginate tubular structure (reaction time was 1 min during preparation). Scale bar: 10 mm.

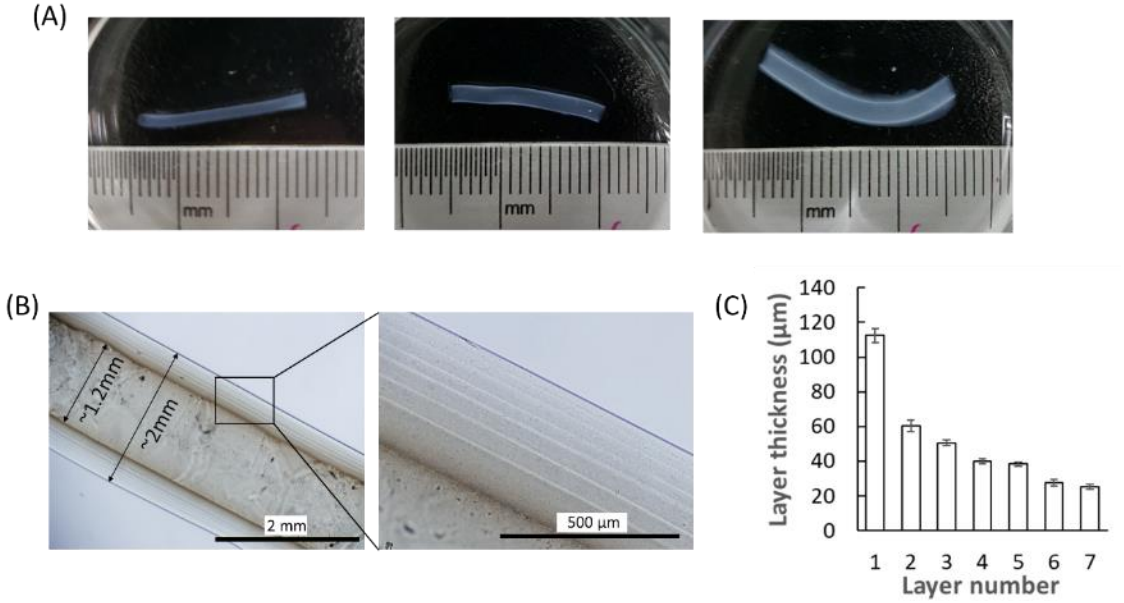

Figure S5. Fabricating small tubular structures. (A) Images of hollow tubes of 1 to 3 mm in diameter. (B) Representative microscopy images of a seven-layer hollow tube of 1.2 mm and 2 mm inner and outer diameters, respectively. (C) Quantification of the thickness of each layer for (B).

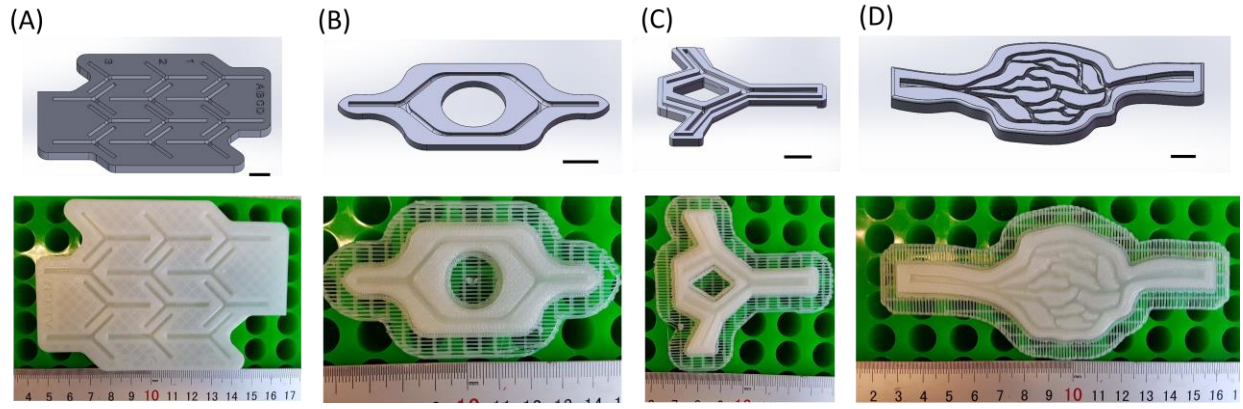

Figure S6. CAD design and corresponding 3D printed custom molds for reversible gel core casting, including (A)-(B) bifurcating, (C) quadrifurcate, and (D) irregular connecting structures. Scale bar: 10 mm.

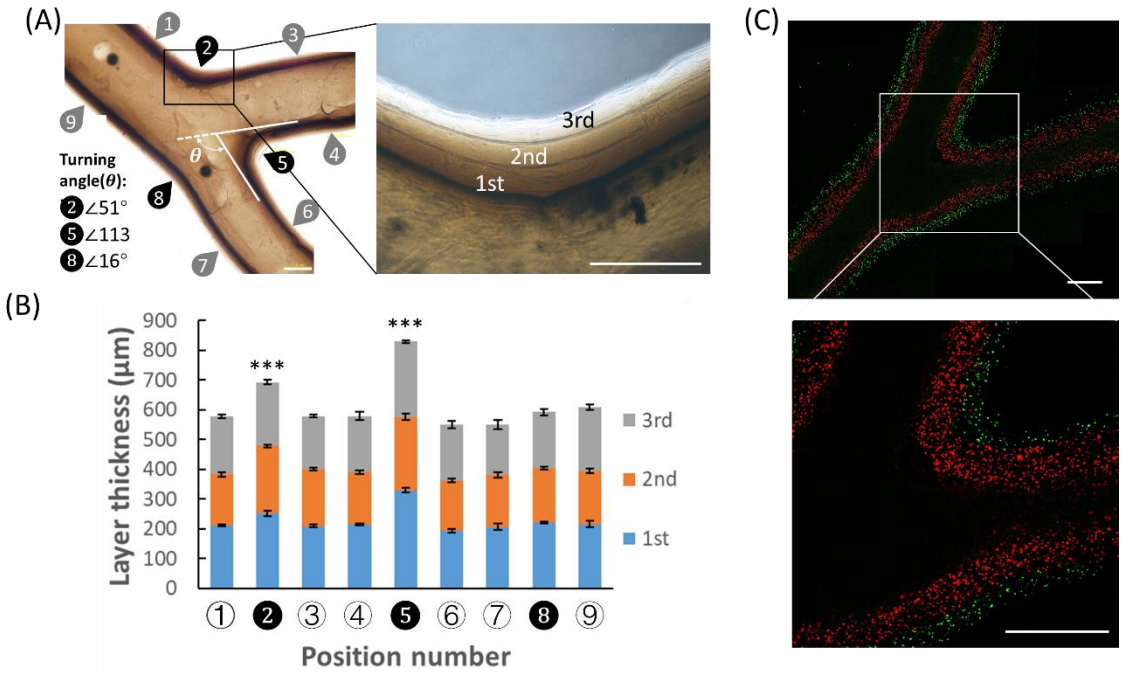

Figure S7. Fabricating multilayer and branched hollow structures. (A) Representative images of a bifurcating tube with three-layer walls, where various positions are marked with numbers. In particular, there are angles at position 2, 5 and 8 of 51°, 113° and 16°, respectively. (B) Quantification of the thicknesses for each layer at the labeled positions. (C) Images of a bifurcating two-layer tube containing fluorescence-tracked cells. Scale bar: 1mm.

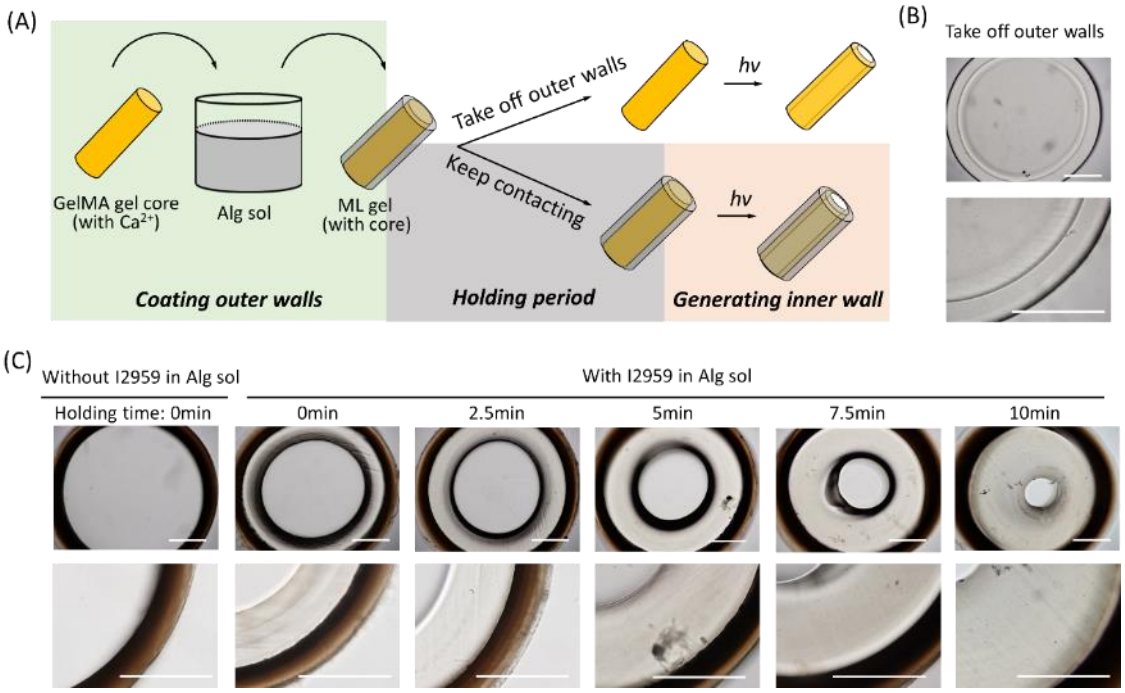

Figure S8. Heterogeneous tube fabrication. (A) Schematic of the photocrosslinking process with two options, where the outer wall is either removed or retained. (B) Cross-section of the inner gel treated with UV after removal of the outer wall. (C) Cross-section images of the heterogeneous hollow tubes under different holding period times. Scale bar: 1mm.

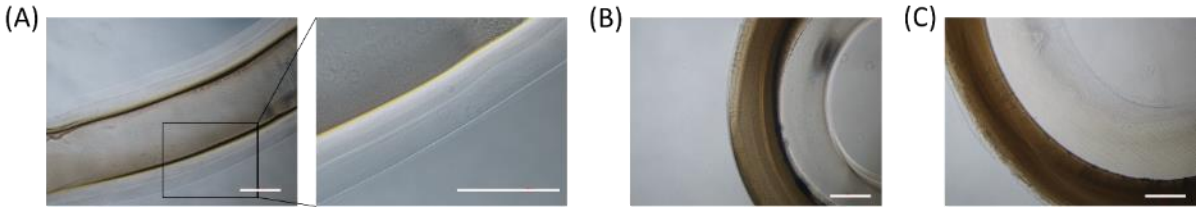

Figure S9. Additional core and photocrosslinking formulations. (A) Images of a two-layer hollow tube using 40% F127 as the reversible gel core materials. Images of a heterogeneous tube using (B) 5% gelatin plus 5% GelMA and (C) 5% gelatin plus 2.5% MeHA as the thermally reversible and photocrosslinkable gel core formulations. Scale bar: 500µm.

Movie S1. Perfusion demonstration of a quadrifurcate vasculature-like structure. DI water supplemented with food dye was perfused through branched hollow channels using syringe.